

Potential Inhibition of ACE2 Membrane Protein by Flavone Glycosides for Blocking Entrance of SARS- CoV-2 into the Cells; a Computational Study

Ahsan Ibrahim*, Ehtisham Ul Haq

Shifa Tameer-e-Millat University, Islamabad-44000, Tel. +9251-8438061 Fax. +9251-8438059, Pakistan.

Corresponding author*

ahsan.scps@stmu.edu.pk

Manuscript received: 07 October, 2022. Revision accepted: 07 December, 2022. Published: 10 January, 2023.

Abstract

Severe acute respiratory syndrome coronavirus 2 (SARS- CoV-2), since its emergence in Wuhan city of China in late 2019, had been a dilemma for the global healthcare system. Humongous efforts have been put in ascertaining the effective treatments for attenuation of the spread of corona virus disease (COVID-19) pandemic. The aim of this research study is to probe the potential inhibition of angiotensin converting enzyme 2 (ACE2) membrane protein by well-known flavone glycosides, hence preventing the binding of spike proteins with ACE2 and subsequent prevention of entry of SARS- CoV-2 inside the cells. The molecular docking analysis, for total ten flavone glycosides was carried out, that laid out propitious results in terms of binding energies towards the active residues of ACE2 protein with a range of -9.3 to -7.1 kcal/mol. The molecular dynamics simulation also yielded promising outcomes. The in-silico toxicity analysis of all the potential drug candidates was carried out that revealed that all the compounds were non-toxic and safe. Studies may be required for optimum formulation development using these compounds as a part of drug discovery and development phenomenon. This study may play a vital part in exploration of natural compounds in pharmacotherapy of COVID-19.

Keywords: ACE2 membrane protein; COVID-19; flavone glycosides; molecular docking analysis; SARS- CoV-2; spike proteins.

Abbreviations:

SARS- CoV-2	: Severe Acute Respiratory Syndrome Coronavirus 2
COVID-19	: Corona Virus Disease
ACE2	: Angiotensin Converting Enzyme 2
ssRNA	: Single Stranded Ribonucleic Acid
PRRAR	: Furin cleavage site in spike protein
TMPRSS2	: Transmembrane Serine Protease 2
S protein	: Spike protein
S cleavage	: Spike cleavage
RBD	: Receptor Binding Domain
PDB	: Protein Data Bank
ADMET	: Absorption, Distribution, Metabolism, Elimination and Toxicity profile

INTRODUCTION

The severe acute respiratory syndrome coronavirus-2 (SARS-CoV-2) emerged as the most common clinical presentation of severe COVID-19 (Brosnahan et al. 2020). Coronavirus disease started in Wuhan, China in late 2019, spreading worldwide, affecting 612 million people and total number of deaths exceeds 6.53 million as of September 2022 as per statistics of World Health Organization (WHO) (“WHO Coronavirus (COVID-19) Dashboard | WHO Coronavirus (COVID-19) Dashboard with Vaccination Data” n.d.). The advent of COVID-19 created serious crisis in health sector, leaving behind huge gaps in the field of disease control and prevention,

that could be bridged through new research and investigations.

The genome of COVID-19 had been the most noteworthy in the ongoing research on SARS- CoV-2. It is a positive sense single-stranded RNA (+ssRNA) and hence tends to replicate in a swift way within the host cell. The genetic material of the virus encodes for many nonstructural proteins (NSPs) that implement enormous functions for virus such as taking the control the host biosynthetic machinery, viral replication, viral protein processing etc. The function of some NSPs is still unknown. The structural genes of this virus encode for the structural proteins, which include spike (S), membrane (M), envelope (E), and nucleocapsid (N) proteins, having a wide spectrum of functions in

characterizing the entry and pathogenicity of the viral particle in the host cell.

The Homotrimers of S proteins make up the spikes on the surface of viral particle and they are involved in the attachment to the host cell receptors. Spike proteins hold prime importance in relation to the ACE2 proteins to which they bind and provoke the infective cascade of COVID-19 (Chen, Liu, and Guo 2020).

In host cells, spike protein (S protein) is cleaved at the furin cleavage site i.e. PRRAR motif by a protease named furin into S1 and S2 to form a heterodimer of S1/S2, which is finally assembled in the form of the trimeric spike protein complex. The S2 subunit of this complex is cleaved by host proteases like transmembrane protease serine 2 (TMPRSS2) to uncover the fusion peptide for membrane fusion of the host cell and virus (Wu et al. 2022). S1 is for binding to the host cell receptor angiotensin-converting enzyme 2 (ACE2). It is V-shaped and the second one (S2 subunit) for fusion of the viral and host cell membranes (Sternberg and Naujokat 2020). ACE2 and TMPRSS2 are abundantly present in the airways, arteries, nasal and oral mucosa, kidneys, the intestine, most profusely expressed on epithelial cells of the respiratory tract i.e. type II pneumocytes that are the cells responsible for secreting surfactant to lessen the surface tension and prevent lung collapse (Sternberg and Naujokat 2020; Akkız 2022). Receptor-binding domain (RBD) contains a receptor binding motif, which is the necessary for spike protein (S1) that binds to the outer surface of ACE2 protein. TMPRSS2 cleaves a part of spike proteins and promote the adhesion of SARS-CoV-2 S protein to get fuse with host cell membrane as the extended spike fosters the fusion of viral and host cell membrane. Subsequently, many hydrophobic amino acids are also generated that get concealed in nearby cell membrane. The virus enters into the cell and have a first encounter with host cell biosynthetic machinery for translation of viral genetic material into viral proteins leading to prompt replication. Cells that overexpress ACE2 and TMPRSS2 are more susceptible to SARS-CoV-2 entry (Akkız 2022; Ahmad et al. 2021).

ACE2 is a membrane-bound carboxydipeptidase protein. ACE2 degrades angiotensin II to generate angiotensin 1-7, which downregulates regulates a variety of angiotensin II actions mediated by counteracting effects against the excessively activated ACE/angiotensin II/AT1R axis, angiotensin II type 1 receptor, as seen in hypertension, cardiac hypertrophy, heart failure, and some cardiovascular disorders. On the other hand, human ACE2 is a known receptor by which SARS-CoV-2 particle enters host cells, by mutual binding of the spike protein of SAR-CoV-2 and ACE2 membrane protein. This makes it a critical site for stopping the SARS- CoV-2 to enter the cells using various ligands. So, it is pivotal to inhibit ACE2, prevent viral genetic material entry into the cell (Kai and Kai

2020). The **figure 1** summarizes the mechanism of the whole process.

Flavonoids are the polyphenolic compounds, very popular for the extensive pharmacological effects they provide such as anti-cancer, anti-inflammatory, antioxidant etc. (Panche, Diwan, and Chandra 2016). Flavones are one of the subclasses of flavonoids. The glycosidic linkages at positions 3 or 7 of flavones leads to formation of flavone glycosides (Kumar and Pandey 2013). Besides various therapeutic effects such as antimicrobial, antidiabetic, hepatoprotective, antitumor and immunomodulatory effects (Xiao et al. 2016), flavone glycosides have also been studied and reported for having antiviral effects against Herpes Simplex Virus (HSV) 1 and 2 (Yarmolinsky et al. 2012).

Keeping in view that fact that ACE2 is a potential target, this study is going to use molecular docking as a tool to inquire regarding the activity of flavone glycosides for inhibiting ACE2 and blocking the entry of SARS- CoV-2 into the cell and arresting the viral replication process.

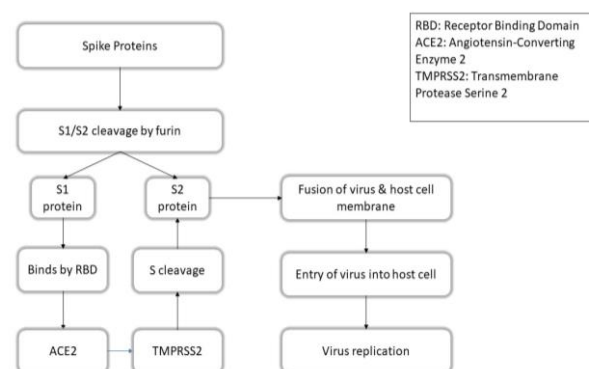


Figure 1. Mechanism of entry of SARS- CoV-2 into the cells through ACE2 membrane protein

MATERIALS AND METHODS

Macromolecule Preparation

The 3D structure of the ACE2 protein was retrieved from RCSB-Protein Data Bank database in PDB format (PDB ID: 1R42) (Towler et al. 2004a). X-Ray crystallography method was used for the determination of the structure of the macromolecule. The macromolecule was prepared by removing the unwanted water molecules, heteroatoms and ligands from the structure of protein on software BIOVIA Discovery Studio Visualizer v17.2.0.16349. The cleaning of protein helps to purely observe the interaction between ligand and the target protein residues, without any influence of these unnecessary entities.

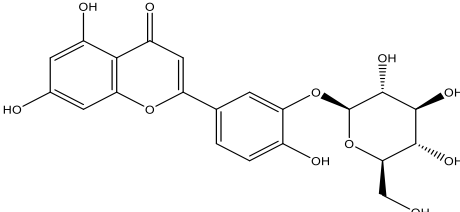
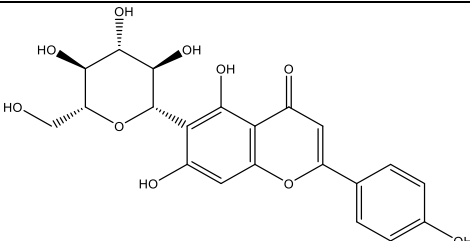
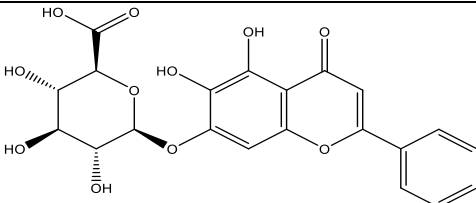
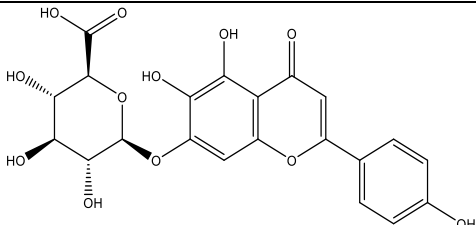
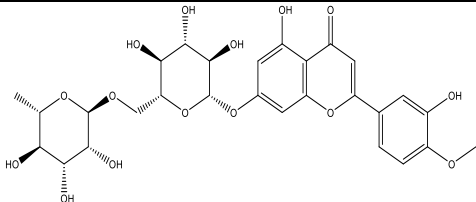
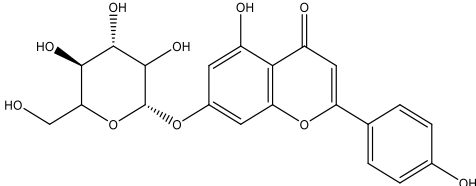
Ligand Preparation

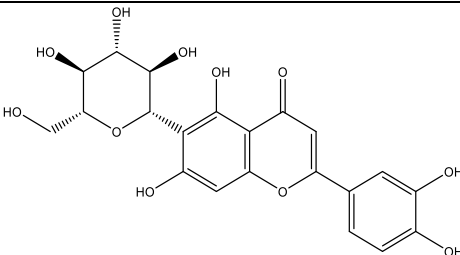
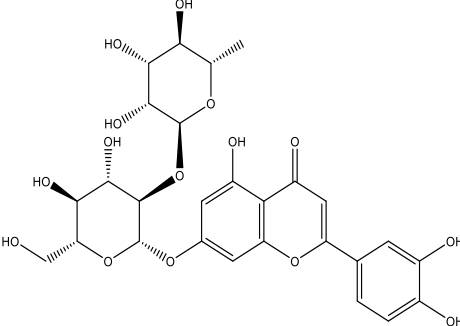
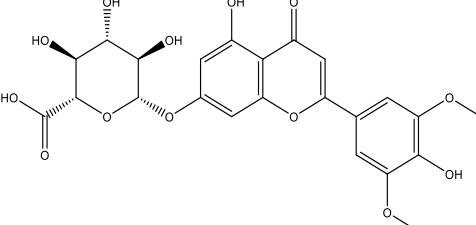
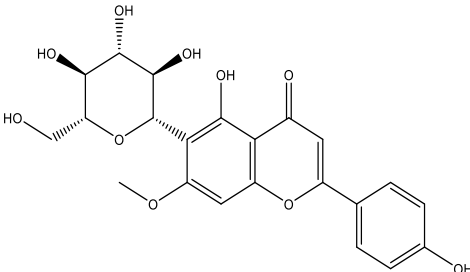
The ligands selected were the flavone glycosides and their structures were acquired from PubChem database.

PerkinElmer Chem 3D 16.0 was used to convert the 3D structure of the ligands into PDB format. Luteolin 3'-glucoside (**L1**), Isovitexin (**L2**), Baicalin (**L3**), Scutellarin (**L4**), Diosmin (**L5**), Apigenin 7-O-glucoside (**L6**), Isoorientin (**L7**), Lonicerin (**L8**), Tricin 7-O-glucouronide (**L9**) and Swertisin (**L10**) were the ligands

used for studying their potential for inhibition of ACE2 protein receptor for preventing the entry of SARS-CoV-2 into the cells containing ACE2 membrane protein, as shown in **table 1**. The two-dimensional structures of the ligands **L1** to **L10** are shown in **figure 2**.

Table 1. The table shows the list of flavone glycoside ligands (L1 to L10) in this study, their chemical structure, botanical source and IUPAC names.

Serial Number	Ligands	PubChem ID	Structure	Botanical Source	Literature Source
L1	Luteolin 3'-glucoside	12309350		<i>Podocarpus nivalis</i>	PubChem
L2	Isovitexin	162350		<i>Carex fraseriana</i>	PubChem
L3	Baicalin	64982		<i>Scutellaria amoena</i>	PubChem
L4	Scutellarin	185617		<i>Scoparia dulcis</i>	PubChem
L5	Diosmin	5281613		<i>Asyneuma argutum</i>	PubChem
L6	Apigenin 7-O-glucoside	44257792		<i>Lonicera japonica</i>	PubChem

Serial Number	Ligands	PubChem ID	Structure	Botanical Source	Literature Source
L7	Isorientin	114776		<i>Carex fraseriana</i>	PubChem
L8	Lonicerin	5282152		<i>Lonicera japonica</i>	PubChem
L9	Tricin 7-O-glucouronide	101939793		<i>Scutellaria discolor</i>	PubChem
L10	Swertisin	124034		<i>Gentiana orbicularis</i>	PubChem

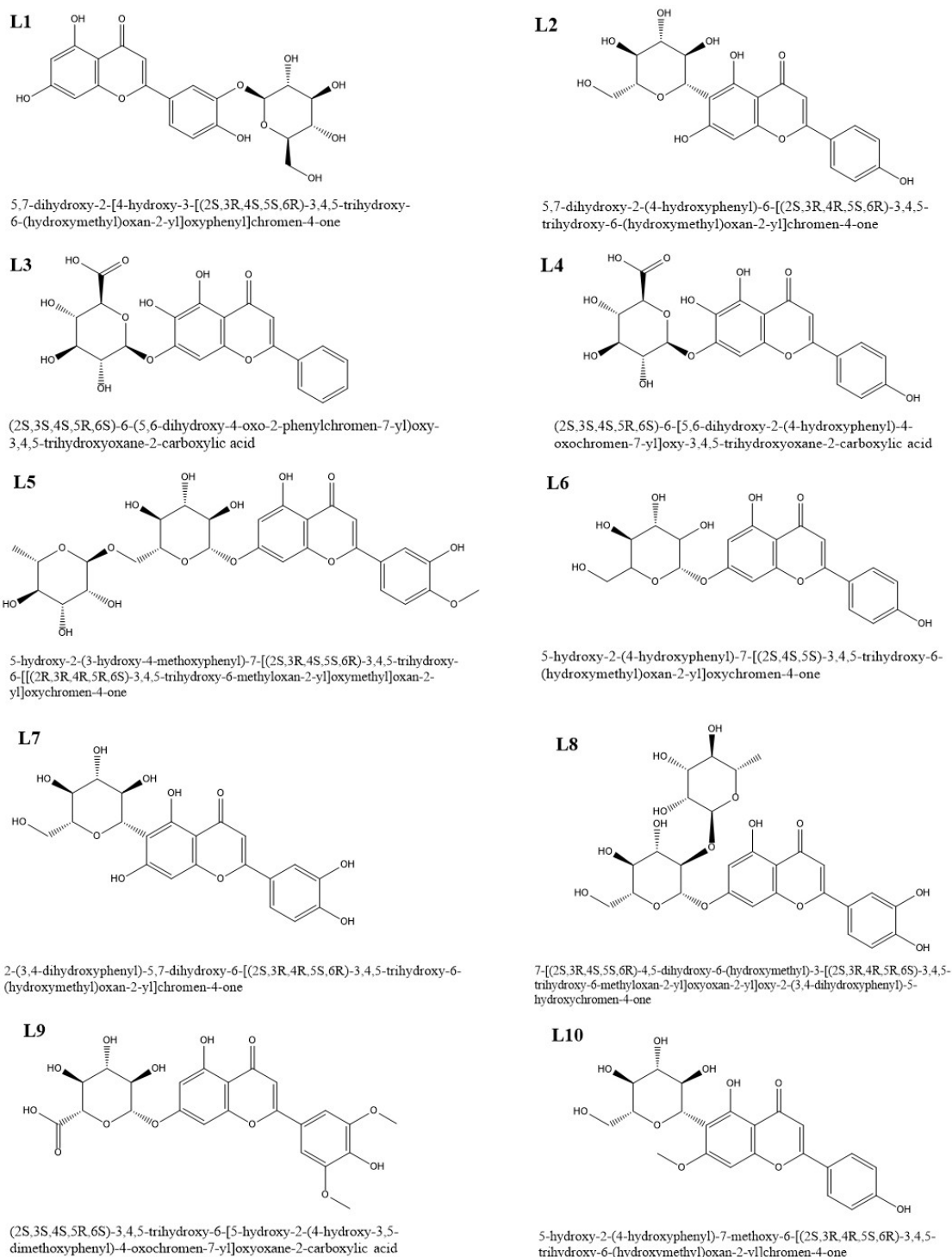


Figure 2. The figure shows the chemical structures of the ligands L1 to L10, along with their IUPAC names obtained from PubChem.

RESULTS AND DISCUSSION

Molecular Docking Analysis & Results

A molecular docking technique has been very handy in drug discovery by pinpointing the drug leads having auspicious therapeutic activity (Ferreira et al. 2015). The molecular docking was performed using PyRx Virtual Screening Tool that is highly reliable as it works on the configuration of Autodock Vina (Ekins, Mestres, and

Testa 2007). For the visualization of protein-ligand interactions, BIOVIA Discovery Studio Visualizer software v17.2.0.16349 was utilized. It provided distinct display of the 2D and 3D interactions along with the bond lengths, aromatic, hydrophobic interactions etc. Promising results were witnessed after the molecular docking analysis of Human ACE2 protein receptor with ligands **L1** to **L10**, as shown in **table 2**.

Table 2. The table shows the findings of the molecular docking and scoring analysis performed for ligands, L1 to L10.

Ligand-Protein Interaction	Binding energy (kcal/mol)	Bonding Residues	Type of bond	Bond Length (Å)	Other Residues
L1	-7.5	His 378	Pi-Pi	5.61	Ala 348, Asp 350, Tyr 385
		His 401	Pi-Pi	4.43	
		Glu 402	Pi- Anion	3.49, 3.75	
L2	-7.1	His 378	Pi-Pi	4.93	Asp 382, Asn 394
		His 401	Pi-Pi	5.71	
		Glu 402	Pi- Anion	4.20	
L3	-8.1	His 401	H bond	2.53	Ser 44, Asp 350, Asp 382
L4	-8.2	His 401	H bond	2.50	Ser 44, Trp 349, Asp 350, Asp 382, Tyr 385
L5	-9.3	His 378	H bond	3.31	Phe 40, Asp 350, Asp 382, Asn 394
		His 401	Pi- Alkyl	5.12	
L6	-7.9	His 401	Pi- Donor H bond	2.58	Ser 44, Ala 348, Trp 349, Asp 350
		Glu 402	H bond	2.38	
L7	-7.4	His 378	Pi-Pi	4.93	Ala 348, Glu 375
		His 401	Pi-Pi	5.72	
L8	-8.4	His 378	Pi-Pi	4.94	Ser 44, Ala 348, Trp 349, Tyr 385, Tyr 515
		Glu 402	Pi-Anion	3.57	
L9	-8.0	Glu 402	H bond	2.11	Trp 349, Asp 350, Arg 514
L10	-7.3	His 378	H bond, Pi-Pi	3.11, 4.95	Pro 346, Asp 382, Arg 393
		His 401	H bond, Pi-Pi	2.53, 5.77	

All the ligands **L1** to **L10**, exhibited their firm interactions with the binding site residues of Human ACE2 protein receptor i.e. His 378, His 401 and His 402 (Towler et al. 2004b), with a binding affinity ranging from -9.3 to -7.1 kcal/mol. The best binding energy of -9.3 kcal/mol was expressed by Diosmin (**L5**), while the binding energies exhibited by other compounds in this study were -8.4 kcal/mol for Lonicerin (**L8**), -8.2 kcal/mol for Scutellarin (**L4**), -8.1 kcal/mol for Baicalin (**L3**), -8.0 kcal/mol for Tricin 7-O-glucouronide (**L9**), -7.9 kcal/mol for Apigenin 7-O-glucoside (**L6**), -7.5 kcal/mol for Luteolin 3'-glucoside (**L1**), -7.4 kcal/mol for Isoorientin (**L7**), -7.3 kcal/mol for Swertisin (**L10**) and -7.1 kcal/mol for Isoviteixin (**L2**).

All the ligands showed absolute interactions with the active site residues of Human ACE2 enzyme. Luteolin 3'-glucoside (**L1**) and Isoviteixin (**L2**) were bound to His 378, His 401 and Glu 402 with considerable binding energies. Ligands, Baicalin (**L3**) and Scutellarin (**L4**)

manifested binding with His 401 residues with shorter bond lengths. Diosmin (**L5**) and Apigenin 7-O-glucoside (**L6**) showed their interactions with His 378, His 401 and His 401, Glu 402 residues, respectively with reasonable bond lengths. Ligands, Isoorientin (**L7**), Lonicerin (**L8**), Tricin 7-O-glucouronide (**L9**) and Swertisin (**L10**), all demonstrated their robust binding affinities with active residues His 378, His 401 and Glu 402 with substantial bond lengths, with Pi-Pi and hydrogen bonds. Strong interactions and short bond lengths also appeared with some other residues i.e. Ser 44, Ala 248, Trp 349 and Asp 350 may also be the active residues of ACE2 protein. The interactions of the best docked ligand Diosmin (**L5**) are shown in **figure 3**. While **figure 4** demonstrates the interactions of top three ligands with highest binding energies (**L5**, **L8** and **L4**) with ACE2 binding site.

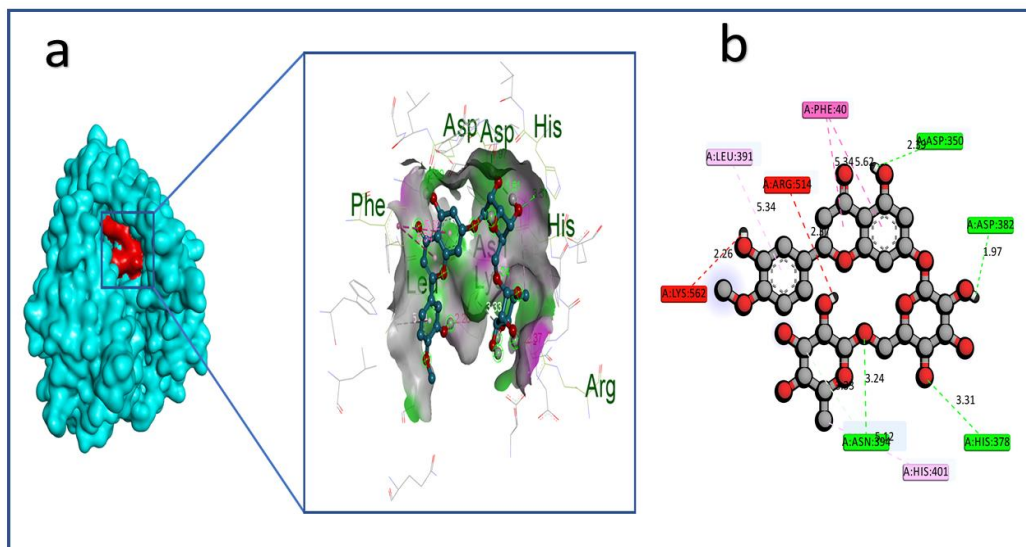


Figure 3. The best docked ligand, Diosmin (L5) blocking the binding site of ACE2 (a) and 2D diagram of interactions of L5 with active site residues (b).

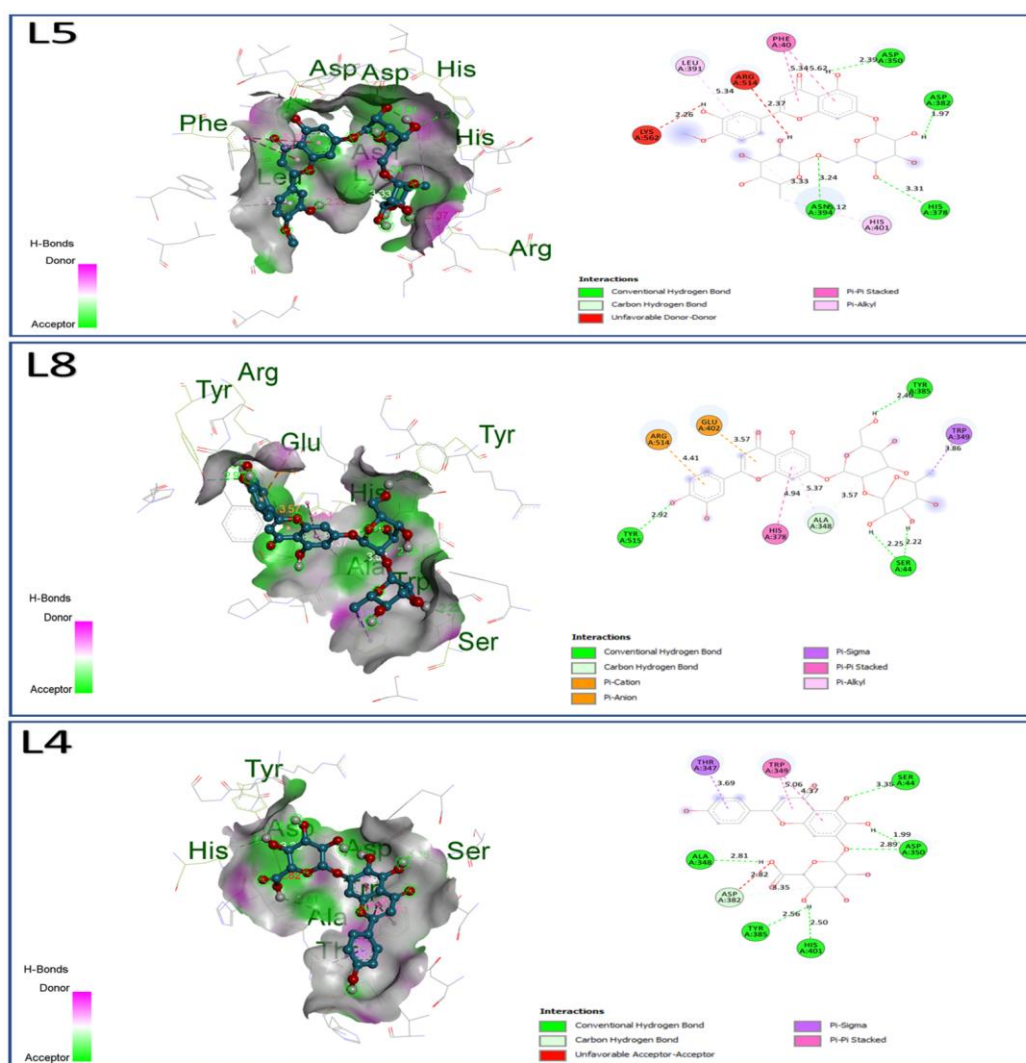


Figure 4. 3D and 2D interactions of top three ligands with respect to binding energies (L5, L8 and L4) respectively, with the active site residues of ACE2 protein.

ADMET Analysis

ADMET profile of a specific ligand serves as a surrogate for its fate to be considered as a potential drug candidate. Swiss ADME was employed for analyzing the ADME profile of the potential drug candidates in this study (Daina, Michielin, and Zoete 2017). Toxicity profile was established through DataWarrior V5.5.0 (Sander et al. 2015). The ORISIS property explorer was used for the prediction of druglikeness score of all potential drug candidates. The molecular weights of ligands from **L1** to **L10** are 448.38, 432.38, 446.36, 462.36, 608.54, 432.38, 448.38, 594.52, 506.41 and 446.40 grams per mole (g/mol), respectively. The highest score for bioavailability was expressed by **L2** and **L10** i.e. 0.55. While **L1**, **L5**, **L7**, **L8** conveyed their bioavailability score as 0.17 and a bioavailability score of 0.11 was predicted for **L3**, **L4** and **L9**. A further *in-vitro* and *in-vivo* studies are recommended for improvement and tailoring of the pharmacokinetic profile of these potential drug candidates, so that these could be formulated in such a way that they may act as potent inhibitors of ACE2 in attenuating SARS-CoV-2. The toxicity profile of these ligands, studied on DataWarrior V5.5.0, was unremarkable for all the

ligands, **L1** to **L10**. The ADMET profile of ligands **L1** to **L10** is shown in **table 3**. The bioavailability radar of Diosmin (**L5**) is provided in the **figure 5**.

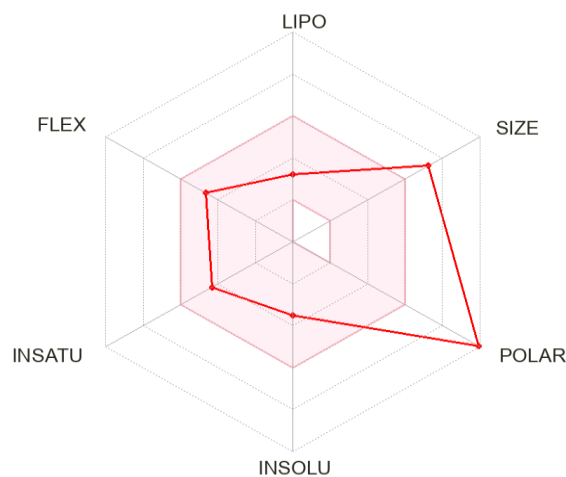


Figure 5. Bioavailability radar of the best docked ligand, Diosmin (**L5**), obtained through SwissADME.

Table 3. The table represents the in-silico profiling of ADMET, Physicochemical properties, Druglikeness and Toxicity of the ligands (L1 to L10)

Drug Candidates	L1	L2	L3	L4	L5	L6	L7	L8	L9	L10
Physicochemical Properties										
Mol.W (g/mol)	448.38	432.38	446.36	462.36	608.54	432.38	448.38	594.52	506.41	446.40
H-Acc	11	10	11	12	15	10	11	15	13	10
H-Don	7	7	6	7	8	6	8	9	6	6
N.R.B	4	3	4	4	7	4	3	6	6	4
TPSA (Å ²)	190.28	181.05	187.12	207.35	238.20	170.05	201.28	249.20	205.58	170.05
Log P	-0.06	0.05	0.22	-0.20	-0.44	0.55	-0.24	-1.03	0.30	0.35
B.Sc	0.17	0.55	0.11	0.11	0.17	0.55	0.17	0.17	0.11	0.55
Drug-likeness										
D.L.S	-3.4	-1.2	0.8	1.04	3.85	-2.3	-0.7	2.4	2.0	-1.1
N.L.V	2	1	2	2	3	1	2	3	3	1
Metabolism										
CYP 1A2	No									
CYP 2C19	No									
CYP 2C9	No									
CYP 2D6	No									
CYP 3A4	No									
P-glycoprotein	No	No	Yes	Yes	Yes	Yes	No	Yes	Yes	No
Toxicity										
Mutagenicity	No									
Tumorigenicity	No									
Irritant	No									
Reproductive Effects	No									

Mol. W (g/mol) Molecular Weight, H-Acc Hydrogen bond Acceptors, H-Don Hydrogen bond Donors, N.R.B Number of Rotable Bonds, TPSA (Å²) Topological Polar Surface Area, Log P prediction of octanol/water

partition coefficient, B.Sc Bioavailability Score, D.L.S Druglikeness score, N.L.V Number of Lipinski's rule violations, CYP Cytochrome P-450 enzyme.

Molecular Dynamics Simulation

The molecular dynamics simulation is performed to assess the physical dynamics or motions of a molecule, virtually on a computer which imparts a lot of details and facts about motions and gestures of a given docked macromolecule complex. The molecular dynamics simulation for the top docked complex of Diosmin (L5) was conducted using iMODS server (López-Blanco, Garzón, and Chacón 2011). The molecular dynamics

simulation was carried upon Normal Mode Analysis (NMA). The results for B-factor or mobility were imparted. This is an important factor of the protein crystallography, which specifies the residues with in the complex that deform themselves to interact with other residues, exposing the flexibility of a molecule. The arrow field around the complex shows the orientation of our complexed macromolecule virtually, as shown in the **figure 6**.

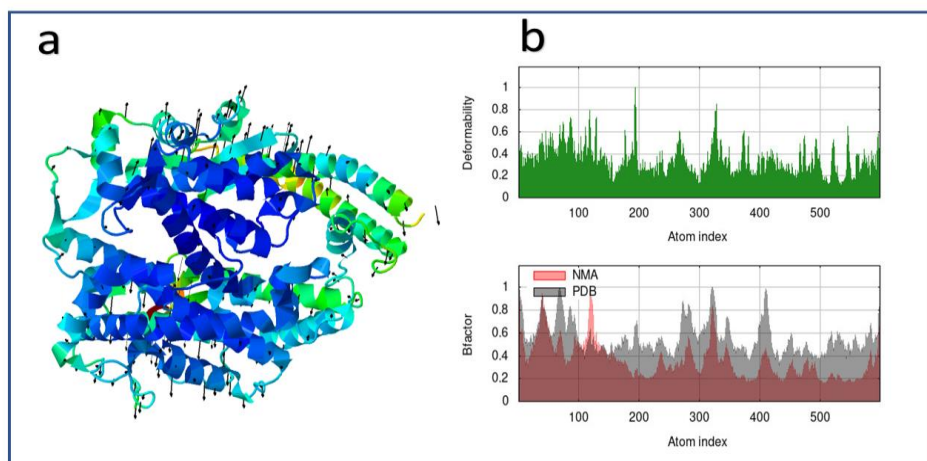


Figure 6. The figure shows the diagrammatic results of the molecular dynamics simulation done with the best docked complex, Diosmin (L5) with ACE2 protein. Image (a) shows the orientation of the docked complex with the arrow field. Image (b) shows the deformability graph and graphical representation of the B-factor.

Eigenvalue was also yielded through this server that denotes the energy required for deforming a residue in a dynamic protein for interaction with other residues. The less is the eigenvalue, the more is the ease for deformation of the residues. The Eigenvalue of the studied complex was $5.6245e-05$. Covariance map casts

a scenario of interactions between the residues of the protein and ligand in the complex while the elastic network deliver a complete picture of the stiffness within the target molecule, hence giving an estimate of deforming in the residues of the target protein, as provided in **figure 7**.

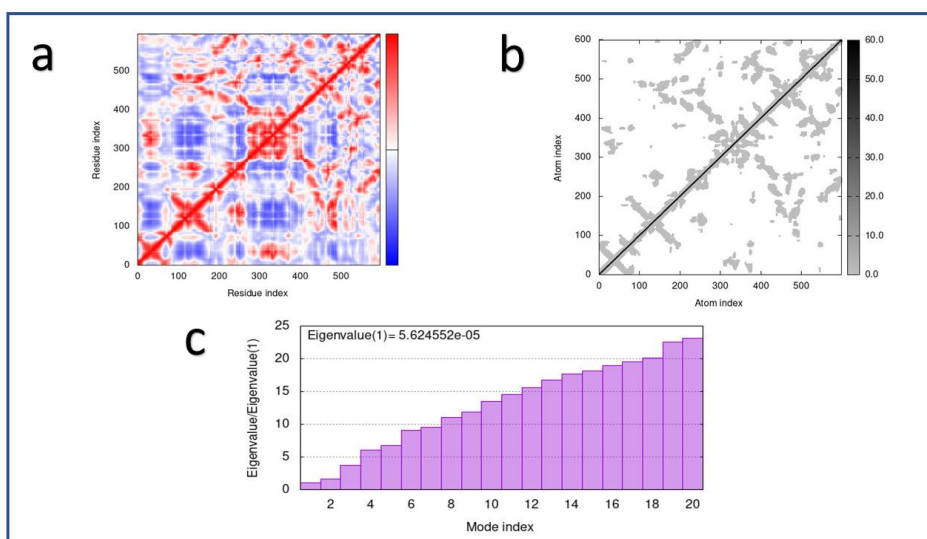


Figure 7. Image (a) demonstrates the covariance graph of the best docked complex Diosmin (L5) and ACE2 protein, Image (b) represents the elastic network map of the docked ligand while Image (c) represents the eigenvalue of the docked ligand.

Discussion

Molecular docking is a worthwhile tool in the drug discovery and repurposing phenomenon in the arena of computer aided drug designing (Hughes et al. 2011). The interaction of a specific compound with a specific target molecule is predicted computationally, without utilizing the wet lab (Meng et al. 2011). In this study, molecular docking was used to recognize the potential inhibition of ACE2 enzyme by flavone glycosides. In this study, it was observed that flavone glycosides had an appreciable range of binding affinities with the active site residues of ACE2 enzyme i.e. -9.3 to -7.1 kcal/mol. The potential drug candidates exhibited their powerful interactions with the active residues of ACE2 i.e. His 378, His 401 and Glu 402. Luteolin 3'-glucoside (**L1**) showed binding energy of -7.5 kcal/mol, that is highly encouraging for inhibition of ACE2. Luteolin 3'-glucoside (**L1**), isolated from *Podocarpus nivalis* ("Luteolin 3'-Glucoside | C21H20O11 - PubChem" n.d.) has also been identified as hepatoprotective and immunoregulatory agent in some studies (Park and Song 2019). Isovitexin (**L2**), acquired from *Carex fraseriana* ("Isovitexin | C21H20O10 - PubChem" n.d.), also spotted for its anti-inflammatory and antidiabetic potential (Abdulai et al. 2021), has provided very optimistic results regarding binding and potential inhibition of ACE2. A reasonable binding energy of -7.1 kcal/mol and linkages with active residues can make a considerable molecule having potential inhibitory activity for ACE2. Baicalin (**L3**) is a flavone glycoside derived from *Scutellaria amoena* ("Baicalin | C21H18O11 - PubChem" n.d.), has anti-inflammatory effects in cardiovascular, neurodegenerative and infectious ailments (Hu et al. 2022), while Scutellarin (**L4**) gained from *Scoparia dulcis* ("Scutellarin | C21H18O12 - PubChem" n.d.), has been reported as to be an antioxidant, antitumor, antiplatelet, cardioprotective and immunomodulatory (Wang and Ma 2018). Both have showed an excellent affinity for ACE2 active residue His 401, with binding energies -8.1 and -8.2 kcal/mol with considerably shorter bond lengths of 2.53 and 2.50 Angstrom, respectively. Diosmin (**L5**) was the potential drug candidate that delivered the most decent results in terms of binding energy, that was -9.3 kcal/mol and was bound to His 378 and His 401. It has been reported that Diosmin (**L5**), obtained from *Achyrocline satureioides* ("Diosmin | C28H32O15 - PubChem" n.d.), works as an antioxidant as well as relieves venous insufficiencies (Feldo et al. 2018). Some studies have revealed that Apigenin 7-O-glucoside (**L6**) from plant *Lonicera japonica* ("Apigenin 7-O-Beta-D-Glucoside | C21H20O10 - PubChem" n.d.), was found to be antimicrobial and cytotoxic (Nie et al. 2018) and this study has detected **L6** as a potential inhibitor of ACE2 with a binding energy of -7.9 kcal/mol with active residues and shorter bond lengths. Isoorientin (**L7**), derived from *Carex fraseriana* ("Isoorientin |

C21H20O11 - PubChem" n.d.), bound to the target with energies of -7.4 kcal/mol and showed potent affinity for active site. A study has outlined the role of Isoorientin (**L7**) in lowering inflammatory mediators, relieving algesia and combating free radicals as well (Yuan et al. 2016). Lonicerin (**L8**), a chemical constituent of *Lonicera japonica* ("Lonicerin | C27H30O15 - PubChem" n.d.), has also been described for its potent anti-pseudomonal pharmacology (Xu et al. 2019). In this study, the binding energy of -8.4 kcal/mol of Lonicerin (**L8**) and its connection with His 378 and Glu 402 tells the possible inhibitory activity for ACE2. Tricin 7-O-glucouronide (**L9**), isolated from *Scutellaria discolor* ("Tricin 7-O-Glucuronide | C23H22O13 - PubChem" n.d.), is known for its inhibition for cervical cancer cell growth through upheld expression of Bax and caspases (Laishram et al. 2015), seems to have a significant potential to bind ACE2 in Human, as per this study, with optimistic energy of -8.0 kcal/mol, with bond length of 2.11 Angstrom with Glu 401. Swertisin (**L10**), a principle component of *Gentiana orbicularis* ("Swertisin | C22H22O10 - PubChem" n.d.), well known for its antioxidant and inflammation fighting tendencies ("Swertisin (CHEBI:131838)" n.d.), came up with a binding energy value of -7.3 kcal/mol and interactions with His 378 and His 401. Hence, all the potential drug candidates have furnished hopeful results in terms of potential inhibition of ACE2 in Human that can be further studied and validated through *in-vitro* and *in-vivo* studies.

The molecular dynamics simulation study clues that the studied complex had a substantial degree of deformability. The low eigenvalue, the covariance map and the elastic network of the studied complex are the evidences of the promising deformability and admissible dynamics of the molecule.

CONCLUSION

In this study, it is concluded that the ligands **L1- L10** have shown a potent activity for ACE2 protein receptor for potentially averting the entry of SARS-CoV-2 into the cells. The ligands have manifested pertinent interactions with ACE2 active residues, showing highly encouraging binding energies. The molecular dynamics simulation studies also provided hopeful results. However, *in-vitro* and *in-vivo* studies are required to confirm these findings. Furthermore, pharmaceutical studies are also recommended for these compounds in formulating them as a suitable drug delivery system for maximal therapeutic efficacy.

COVID-19 had been very grim challenge for the health system around the globe. The focus of the ongoing research in the field of drug discovery revolves around the drug development for COVID-19. Many concerns have developed in terms of efficacy as well as safety for many drugs to be used against this virus. On

the basis of findings of this study, an inference could be drawn that these flavone glycosides could be utilized as potential drug molecules for restricting the entry of SARS-CoV-2 entry into the cells they infect by blocking ACE2 receptor protein, especially in lungs. This study will assist the researchers for preclinical and clinical investigation of these potential drug molecules.

Acknowledgement: The study is carried out entirely by the authors, so there is no need for acknowledgement.

Authors' Contributions: Example: Ahsan Ibrahim designed the study. Ahsan Ibrahim carried out the computational work. Ahsan Ibrahim & Ehtisham Ul Haq wrote the manuscript. All authors read and approved the final version of the manuscript

Competing Interests: There exist no competing interests.

REFERENCES

- Abdulai, Ibrahim Luru, Samuel Kojo Kwofie, Winfred Seth Gbewonyo, Daniel Boison, Joshua Buer Puplampu, and Michael Buenor Adinortey. 2021. "Multitargeted Effects of Vitexin and Isovixetin on Diabetes Mellitus and Its Complications." *The Scientific World Journal* 2021. <https://doi.org/10.1155/2021/6641128>.
- Ahmad, Iqrar, Rahul Pawara, Sanjay Surana, and Harun Patel. 2021. "The Repurposed ACE2 Inhibitors: SARS-CoV-2 Entry Blockers of Covid-19." *Topics in Current Chemistry (Cham)* 379 (6). <https://doi.org/10.1007/S41061-021-00353-7>.
- Akkız, Hikmet. 2022. "The Biological Functions and Clinical Significance of SARS-CoV-2 Variants of Concern." *Frontiers in Medicine* 9 (May). <https://doi.org/10.3389/FMED.2022.849217>.
- "Apigenin 7-O-Beta-D-Glucoside | C21H20O10 - PubChem." n.d. Accessed September 13, 2022. <https://pubchem.ncbi.nlm.nih.gov/compound/Apigenin-7-O-beta-D-glucoside>.
- "Baicalin | C21H18O11 - PubChem." n.d. Accessed September 13, 2022. <https://pubchem.ncbi.nlm.nih.gov/compound/Baicalin>.
- Brosnahan, Shari B., Annemijn H. Jonkman, Matthias C. Kugler, John S. Munger, and David A. Kaufman. 2020. "COVID-19 and Respiratory System Disorders: Current Knowledge, Future Clinical and Translational Research Questions." *Arteriosclerosis, Thrombosis, and Vascular Biology* 40 (11): 2586–97. <https://doi.org/10.1161/ATVBAHA.120.314515>.
- Chen, Yu, Qianyun Liu, and Deyin Guo. 2020. "Emerging Coronaviruses: Genome Structure, Replication, and Pathogenesis." *Journal of Medical Virology* 92 (4): 418–23. <https://doi.org/10.1002/JMV.25681>.
- Daina, Antoine, Olivier Michielin, and Vincent Zoete. 2017. "SwissADME: A Free Web Tool to Evaluate Pharmacokinetics, Drug-Likeness and Medicinal Chemistry Friendliness of Small Molecules." *Scientific Reports* 2017 7:1 7 (1): 1–13. <https://doi.org/10.1038/srep42717>.
- "Diosmin | C28H32O15 - PubChem." n.d. Accessed September 13, 2022. <https://pubchem.ncbi.nlm.nih.gov/compound/Diosmin>.
- Ekins, S., J. Mestres, and B. Testa. 2007. "In Silico Pharmacology for Drug Discovery: Methods for Virtual Ligand Screening and Profiling." *British Journal of Pharmacology* 152 (1): 9–20. <https://doi.org/10.1038/SJ.BJP.0707305>.
- Feldo, Marcin, Michał Woźniak, Magdalena Wójciak-Kosior, Ireneusz Sowa, Agata Kot-Waśik, Justyna Aszyk, Jacek Bogucki, Tomasz Zubilewicz, and Anna Bogucka-Kocka. 2018. "Influence of Diosmin Treatment on the Level of Oxidative Stress Markers in Patients with Chronic Venous Insufficiency." *Oxidative Medicine and Cellular Longevity* 2018. <https://doi.org/10.1155/2018/2561705>.
- Ferreira, Leonardo G., Ricardo N. dos Santos, Glaucius Oliva, and Adriano D. Andricopulo. 2015. "Molecular Docking and Structure-Based Drug Design Strategies." *Molecules* 2015, Vol. 20, Pages 13384-13421 20 (7): 13384–421. <https://doi.org/10.3390/MOLECULES200713384>.
- Hughes, J. P., S. S. Rees, S. B. Kalindjian, and K. L. Philpott. 2011. "Principles of Early Drug Discovery." *British Journal of Pharmacology* 162 (6): 1239. <https://doi.org/10.1111/J.1476-5381.2010.01127.X>.
- Hu, Zhihua, Yurong Guan, Wanying Hu, Zhiyong Xu, and Muhammad Ishfaq. 2022. "An Overview of Pharmacological Activities of Baicalin and Its Aglycone Baicalein: New Insights into Molecular Mechanisms and Signaling Pathways." *Iranian Journal of Basic Medical Sciences* 25 (1): 14. <https://doi.org/10.22038/IJBMS.2022.60380.13381>.
- "Isoorientin | C21H20O11 - PubChem." n.d. Accessed September 13, 2022. <https://pubchem.ncbi.nlm.nih.gov/compound/Isoorientin>.
- "Isovitexin | C21H20O10 - PubChem." n.d. Accessed September 13, 2022. <https://pubchem.ncbi.nlm.nih.gov/compound/Isovitexin>.
- Kai, Hisashi, and Mamiko Kai. 2020. "Interactions of Coronaviruses with ACE2, Angiotensin II, and RAS Inhibitors—Lessons from Available Evidence and Insights into COVID-19." *Hypertension Research* 2020 43:7 43 (7): 648–54. <https://doi.org/10.1038/s41440-020-0455-8>.
- Kumar, Shashank, and Abhay K. Pandey. 2013. "Chemistry and Biological Activities of Flavonoids: An Overview." *The Scientific World Journal* 2013. <https://doi.org/10.1155/2013/162750>.
- Laishram, Surbala, Dinesh Singh Moirangthem, Jagat Chandra Borah, Bikas Chandra Pal, Pankaj Suman, Satish Kumar Gupta, Mohan Chandra Kalita, and Narayan Chandra Talukdar. 2015. "Chrysin Rich Scutellaria Discolor Colebr. Induces Cervical Cancer Cell Death via the Induction of Cell Cycle Arrest and Caspase-Dependent Apoptosis." *Life Sciences* 143 (December): 105–13. <https://doi.org/10.1016/J.LFS.2015.10.035>.
- "Lonicerin | C27H30O15 - PubChem." n.d. Accessed September 13, 2022. <https://pubchem.ncbi.nlm.nih.gov/compound/Lonicerin>.
- López-Blanco, José Ramón, José Ignacio Garzón, and Pablo Chacón. 2011. "IMod: Multipurpose Normal Mode Analysis in Internal Coordinates." *Bioinformatics (Oxford, England)* 27 (20): 2843–50. <https://doi.org/10.1093/BIOINFORMATICS/BTR497>.
- "Luteolin 3'-Glucoside | C21H20O11 - PubChem." n.d. Accessed September 13, 2022.

- <https://pubchem.ncbi.nlm.nih.gov/compound/Luteolin-3-glucoside>.
- Meng, Xuan-Yu, Hong-Xing Zhang, Mihaly Mezei, and Meng Cui. 2011. "Molecular Docking: A Powerful Approach for Structure-Based Drug Discovery." *Current Computer-Aided Drug Design* 7 (2): 146. <https://doi.org/10.2174/157340911795677602>.
- Nie, Juan, Hong-Mei Yang, Chao-Yue Sun, Yan-Lu Liu, Jian-Yi Zhuo, Zhen-Biao Zhang, Xiao-Ping Lai, Zi-Ren Su, and Yu-Cui Li. 2018. "Scutellarin Enhances Antitumor Effects and Attenuates the Toxicity of Bleomycin in H22 Ascites Tumor-Bearing Mice." *Frontiers in Pharmacology* 9: 615. <https://doi.org/10.3389/FPHAR.2018.00615>.
- Panche, A. N., A. D. Diwan, and S. R. Chandra. 2016. "Flavonoids: An Overview." *Journal of Nutritional Science* 5 (January): 1–15. <https://doi.org/10.1017/JNS.2016.41>.
- Park, Chung Mu, and Young Sun Song. 2019. "Luteolin and Luteolin-7-O-Glucoside Protect against Acute Liver Injury through Regulation of Inflammatory Mediators and Antioxidative Enzymes in GalN/LPS-Induced Hepatic ICR Mice." *Nutrition Research and Practice* 13 (6): 473. <https://doi.org/10.4162/NRP.2019.13.6.473>.
- Sander, Thomas, Joel Freyss, Modest von Korff, and Christian Rufener. 2015. "DataWarrior: An Open-Source Program for Chemistry Aware Data Visualization and Analysis." *Journal of Chemical Information and Modeling* 55 (2): 460–73. <https://doi.org/10.1021/CI500588J>.
- "Scutellarin | C21H18O12 - PubChem." n.d. Accessed September 13, 2022. <https://pubchem.ncbi.nlm.nih.gov/compound/Scutellarin>.
- Sternberg, Ariane, and Cord Naujokat. 2020. "Structural Features of Coronavirus SARS-CoV-2 Spike Protein: Targets for Vaccination." *Life Sciences* 257 (September): 118056. <https://doi.org/10.1016/J.LFS.2020.118056>.
- "Swertisin | C22H22O10 - PubChem." n.d. Accessed September 13, 2022. <https://pubchem.ncbi.nlm.nih.gov/compound/Swertisin>.
- "Swertisin (CHEBI:131838)." n.d. Accessed September 15, 2022. <https://www.ebi.ac.uk/chebi/chebiOntology.do?chebiId=CHEBI:131838>.
- Towler, Paul, Bart Staker, Sridhar G. Prasad, Saurabh Menon, Jin Tang, Thomas Parsons, Dominic Ryan, et al. 2004a. "ACE2 X-Ray Structures Reveal a Large Hinge-Bending Motion Important for Inhibitor Binding and Catalysis." *The Journal of Biological Chemistry* 279 (17): 17996–7. <https://doi.org/10.1074/JBC.M311191200>.
- _____. 2004b. "ACE2 X-Ray Structures Reveal a Large Hinge-Bending Motion Important for Inhibitor Binding and Catalysis." *The Journal of Biological Chemistry* 279 (17): 17996–7. <https://doi.org/10.1074/JBC.M311191200>.
- "Tricin 7-O-Glucuronide | C23H22O13 - PubChem." n.d. Accessed September 13, 2022. <https://pubchem.ncbi.nlm.nih.gov/compound/Tricin-7-O-glucuronide>.
- Wang, Liping, and Qiang Ma. 2018. "Clinical Benefits and Pharmacology of Scutellarin: A Comprehensive Review." *Pharmacology & Therapeutics* 190 (October): 105–27. <https://doi.org/10.1016/J.PHARMTHERA.2018.05.006>.
- "WHO Coronavirus (COVID-19) Dashboard | WHO Coronavirus (COVID-19) Dashboard with Vaccination Data." n.d. Accessed September 21, 2022. <https://covid19.who.int/>.
- Wu, Can rong, Wan chao Yin, Yi Jiang, and H. Eric Xu. 2022. "Structure Genomics of SARS-CoV-2 and Its Omicron Variant: Drug Design Templates for COVID-19." *Acta Pharmacologica Sinica* 2022, January, 1–13. <https://doi.org/10.1038/s41401-021-00851-w>.
- Xiao, Jianbo, Esra Capanoglu, Amir Reza Jassbi, and Anca Miron. 2016. "Advance on the Flavonoid C-Glycosides and Health Benefits." *Critical Reviews in Food Science and Nutrition* 56 Suppl 1 (July): S29–45. <https://doi.org/10.1080/10408398.2015.1067595>.
- Xu, Zhongren, Kun Li, Taowen Pan, Jing Liu, Bin Li, Chuanxun Li, Shouyu Wang, Yunpeng Diao, and Xinguang Liu. 2019. "Lonicerin, an Anti-AlgE Flavonoid against Pseudomonas Aeruginosa Virulence Screened from Shuanghuanglian Formula by Molecule Docking Based Strategy." *Journal of Ethnopharmacology* 239 (July): 111909. <https://doi.org/10.1016/J.JEP.2019.111909>.
- Yarmolinsky, Ludmila, Mahmoud Huleihel, Michele Zaccari, and Shimon Ben-Shabat. 2012. "Potent Antiviral Flavone Glycosides from Ficus Benjamina Leaves." *Fitoterapia* 83 (2): 362–67. <https://doi.org/10.1016/J.FITOTE.2011.11.014>.
- Yuan, Li, Jing Wang, Wanqiang Wu, Qian Liu, and Xuebo Liu. 2016. "Effect of Isoorientin on Intracellular Antioxidant Defence Mechanisms in Hepatoma and Liver Cell Lines." *Biomedicine & Pharmacotherapy = Biomedecine & Pharmacotherapie* 81 (July): 356–62. <https://doi.org/10.1016/J.BIOPHA.2016.04.025>.